

Synthesis and Characterization of a New Quasi-One-Dimensional Copper(II) Phosphate, $\text{Ba}_2\text{Cu}(\text{PO}_4)_2$

Kristen M. S. Etheredge[†] and Shiou-Jyh Hwu^{*,*‡}

Departments of Chemistry, Rice University, P.O. Box 1892, Houston, Texas 77251, and
Clemson University, Clemson, South Carolina 29634

Received September 18, 1995[⊗]

Crystals of $\text{Ba}_2\text{Cu}(\text{PO}_4)_2$ have been grown in a low-temperature eutectic flux of 32% KCl and 68% CuCl (mp = 140 °C). The X-ray single-crystal structure analysis shows that this barium copper(II) phosphate crystallizes in a monoclinic lattice with $a = 12.160(4)$ Å, $b = 5.133(4)$ Å, $c = 6.885(4)$ Å, $\beta = 105.42(4)^\circ$, and $V = 414.3(4)$ Å³; $C2/m$ (No. 12); $Z = 2$. The structure has been refined by the least-squares method to a final solution with $R = 0.020$, $R_w = 0.026$, and $\text{GOF} = 1.05$. The framework of the title compound consists of $[\text{Cu}(\text{PO}_4)_2]_\infty$ linear chains with Ba^{2+} cations residing between these parallel chains. The chains are composed of an array of Cu^{2+} cations that are doubly bridged by PO_4 anions. Each pair of bridging PO_4 tetrahedra are in a staggered configuration above and below the CuO_4 square plane, resulting in a linear chain with a long Cu---Cu separation distance, 5.13 Å ($\equiv b$). This quasi-one-dimensional framework is unusual among the Cu^{2+} -based phosphates. Magnetic susceptibility data shows Curie–Weiss paramagnetic behavior in the range of ca. 190–300 K and a possible antiferro-to-ferromagnetic transition at ~ 8 K. In this paper, the synthesis, structure, and properties of the title compound are presented. A structural comparison to a closely related vanadyl $(\text{VO})^{2+}$ phosphate, $\text{Ba}_2(\text{VO})(\text{PO}_4)_2 \cdot \text{H}_2\text{O}$, as well as $\text{Na}_2\text{CuP}_2\text{O}_7$ will be discussed.

Introduction

Fruitful structural chemistry has resulted from the exploratory synthesis of new transition metal phosphate, silicate, and arsenate compounds by employing low-melting halide fluxes.^{1–4} Synthetic techniques other than traditional, high-temperature, solid state synthesis allow new discoveries to be made through altered reaction conditions: acidity/basicity, solubility, and reaction temperature. In our recent studies, we have investigated the chemistry associated with some early transition metals,^{1,2} Ti, V, and Nb, and also one late transition metal, Cu.^{3,4} Copper(II)-based structural chemistry offers an extra dimension of interest and complexity due to the structural multiplicity attributed to the Jahn–Teller distortion (d^9). The distorted CuO_{6-x} ($x = 0–2$) polyhedra share corners and/or edges with the phosphate tetrahedra, allowing unique copper phosphate frameworks to form. Recently, an extended $[\text{CuP}_2\text{O}_7]_\infty$ ribbon structure, which consists of alternating, corner-shared CuO_4 and P_2O_7 units has been reported in the $\text{A}_2\text{CuP}_2\text{O}_7$ ($\text{A} = \text{Li},^5 \text{Na}^{3a}$) family. The honeycomb-like $[\text{BaCl}][\text{CuPO}_4]^{3b}$ structure exhibits an unusual $[\text{CuPO}_4]_\infty$ spiral framework, in that each CuO_4 square plane shares an edge with one PO_4 group and two corners with two different PO_4 groups. In the title compound, the structure

possesses an interesting $[\text{Cu}(\text{PO}_4)_2]_\infty$ linear chain framework formed by corner-shared CuO_4 and PO_4 groups.

The pseudo-one-dimensional $[\text{Cu}(\text{PO}_4)_2]_\infty$ chain structure is unique in the sense that it has not previously been observed in a large collection of copper(II) phosphates (as cited in ref 3a). Additionally, this chain structure has not been observed in isomorphous compounds, for example, $\text{Sr}_2\text{Ni}(\text{PO}_4)_2$.⁶ However, the title compound does have a close structural relationship with a vanadium(IV) compound, $\text{Ba}_2(\text{VO})(\text{PO}_4)_2 \cdot \text{H}_2\text{O}$,⁷ which was also isolated at low-temperature, but in a hydrothermal reaction. The 1D $[(\text{VO})^{2+}(\text{PO}_4)_2 \cdot \text{H}_2\text{O}]_\infty$ vanadyl chain adopts a similar polyhedral connectivity in that VO_6 and PO_4 groups are corner-shared. A structural comparison with $\text{Ba}_2(\text{VO})^{2+}(\text{PO}_4)_2 \cdot \text{H}_2\text{O}$, as well as $\text{Na}_2\text{CuP}_2\text{O}_7$ will be briefly discussed.

Experimental Section

Synthesis. Light blue crystals of $\text{Ba}_2\text{Cu}(\text{PO}_4)_2$ were grown by a two-step process. Initially, the precursor, $\text{Ba}_2\text{P}_2\text{O}_7$, was prepared in an alumina crucible by calcining a stoichiometric mixture of $(\text{NH}_4)_2\text{HPO}_4$ (Aldrich, 98+%), and BaCO_3 (Aesar, 99.9%) in air at 575 °C. Next, a stoichiometric amount of CuO (Strem, 99.9999%) and Cu_2O (Aldrich, 97%) was added to the barium phosphate precursor preparing a reaction mixture with nominal composition of $\text{Ba}_2\text{Cu}_4\text{P}_2\text{O}_{10}$. An eutectic flux of 32% KCl (EM Science, 99.9%) and 68% CuCl (Aldrich, 99+%), mp = 140 °C,⁸ was employed with a flux to charge ratio of 5:1 for the crystal growth experiment. The mixture was placed in an evacuated, carbon-coated, silica ampule and heated at 500 °C for 8 days, cooled at 1 °C/h to 150 °C and then furnace cooled to room temperature. Chunk crystals of the title compound (10% yield) were isolated manually and washed with deionized water using the suction filtration method. The reaction product shows no crystalline material, except the blue phase of $\text{Ba}_2\text{Cu}(\text{PO}_4)_2$, before washing.

[†] Rice University.

^{*} Clemson University.

[⊗] Abstract published in *Advance ACS Abstracts*, February 15, 1996.

- (1) Wang, S.; Hwu, S.-J. *J. Am. Chem. Soc.* **1992**, *114*, 6920. (b) Wang, S.; Hwu, S.-J. *Inorg. Chem.* **1995**, *34*, 166. (c) Wang, S.; Hwu, S.-J.; Paradis, J. A.; Whangbo, M.-H. *J. Am. Chem. Soc.* **1995**, *117*, 5515. (d) Wang, S. Ph.D. Dissertation, Rice University, 1993.
- (2) (a) Serra, D. L.; Hwu, S.-J. *J. Solid State Chem.* **1992**, *101*, 32. (b) Serra, D. L. Ph.D. Dissertation, Rice University, 1993.
- (3) (a) Etheredge, K. M. S.; Hwu, S.-J. *Inorg. Chem.* **1995**, *34*, 1495. (b) Etheredge, K. M. S.; Hwu, S.-J. *Inorg. Chem.* **1995**, *34*, 3123. (c) Etheredge, K. M. S.; Hwu, S.-J. *Inorg. Chem.* **1995**, *34*, 5013.
- (4) (a) Wardojo, T. A.; Hwu, S.-J. *J. Solid State Chem.* **1995**, *118*, 280. (b) Wardojo, T. A. M.A. Thesis, Rice University, 1996.
- (5) Spirlet, M. R.; Rebizant, J.; Liegeois-Duyckaerts, M. *Acta Crystallogr.* **1993**, *C49*, 209.

(6) Ebali, B.; Boukhari, A. *Acta Crystallogr.* **1993**, *C49*, 1131.

(7) Harrison, W. T. A.; Lim, S. C.; Vaughney, J. T.; Jacobsen, A. J.; Goshorn, D. P.; Johnson, J. W. *J. Solid State Chem.*, **1995**, *113*, 444.

(8) Levin, E. M.; Robbins, C. R.; McMurdie, H. F. *Phase Diagrams for Ceramists*; The American Ceramic Society, Inc.: Columbus, OH, 1964; Figure 1243.

Table 1. Crystallographic Data for Ba₂Cu(PO₄)₂

chem formula	Ba ₂ Cu(P ₂ O ₄) ₂	fw	528.16
<i>a</i> , Å	12.160(4)	space group	C2/m (No. 12)
<i>b</i> , Å	5.133(4)	<i>T</i> , °C	23
<i>c</i> , Å	6.885(4)	<i>λ</i> , Å	0.71069
<i>β</i> , deg	105.42(4)	<i>ρ</i> _{calcd} , g cm ⁻³	4.233
<i>V</i> , Å ³	414.3(4)	linear abs coeff, cm ⁻¹	123.490
<i>Z</i>	4		
<i>R</i> ^a	0.020		
<i>R</i> _w ^b	0.026		

$$^a R = \sum[|F_o| - |F_c|]/\sum|F_o|. \quad ^b R_w = [\sum w(|F_o| - |F_c|)^2/\sum w|F_o|^2]^{1/2}.$$

Bulk quantity Ba₂Cu(PO₄)₂ was prepared using the same precursor as above; Ba₂P₂O₇ was combined with a stoichiometric amount of CuO and heated in air over 24 h to 750 °C, heated over 12 h to 775 °C, held for 3 days, and then carefully heated to 785 °C (to avoid overheating, see the thermal analysis section below) and again held for 4 days as the reaction went to completion. The powder X-ray diffraction patterns were taken as previously described, showing no extra reflections due to impurities.^{3a} NIST Si powder was used as internal standard. A total of 14 peaks were indexed and refined by the least-squares program LATT.⁹ The refined cell constants were *a* = 12.176(7) Å, *b* = 5.129(2) Å, *c* = 6.881(5) Å, and *β* = 105.46(7)°, which are in good agreement with the indices found from single crystal data.

Structure Determination. A light blue, chunk crystal was mounted on a glass fiber for single-crystal X-ray diffraction study. The diffraction data were collected at room temperature on a Rigaku AFC5S four-circle diffractometer. Crystallographic data for the title compound are summarized in Table 1. The unit cell parameters and the orientation matrix were determined by a least-squares fit of 25 peak maxima with 7° < 2θ < 30°. A total of 1139 reflections (2θ_{max} = 55°) were collected at room temperature from two octants (*h*, *k*, ±*l*), of which 475 reflections with *I* > 3σ were used for the structure solution. There was no detectable decay during data collection, according to the intensities of three standard reflections (−3, −1, 0; −4, 0, 1; −4, −2, 1) which were measured every 150 reflections. The TEXSAN software package¹⁰ was used for crystal structure solution and refinement. Data reduction, intensity analysis, and extinction conditions were determined with the program PROCESS. Lorentz–polarization and empirical absorption corrections based on two computer chosen azimuthal scans (2θ = 15.92, 32.16°) were applied to the data. On the basis of extinction conditions and correct structure solution, space group C2/m (No. 12) was unambiguously chosen.¹¹ The atomic coordinates of Ba, Cu, and P were determined using the SHELXS-86¹² program, and those of oxygen atoms were resolved by using a difference Fourier map. The structural and thermal parameters were refined by the full-matrix least-squares method to *R* = 0.020, *R*_w = 0.026, and GOF = 1.05. Table 2 lists the final positional and thermal parameters.

Thermal Analysis. Differential thermal analysis (DTA) was carried out on a DuPont 9900 thermal analysis system with a heating rate of 10 °C/min in the temperature range 25–1000 °C. The experiments were done on the polycrystalline sample prepared above in a fused quartz ampule. The DTA shows an inconsistent heating and cooling behavior, suggesting a decomposition which occurs between ~795 and ~810 °C. The DTA product was green in color and unable to be identified by PXRD.

- (9) LATT. Takusagawa, F. Ames Laboratory, Iowa State University, Ames, IA, Unpublished research, 1981.
- (10) TEXSAN: Single Crystal Structure Analysis Software, Version 5.0, Molecular Structure Corp., The Woodlands, TX (1989). (b) Cromer, D. T.; Waber, J. T. Scattering Factors for Non-hydrogen Atoms. In *International Table for X-ray Crystallography*; Kynoch Press: Birmingham, England, 1974; Vol. IV, Table 2.2A, pp 71–98.
- (11) The structure was originally refined in the space group C2, giving rise to *R* = 0.020, *R*_w = 0.025, and GOF = 1.03. The existence of several nonpositive definite temperature factors led to further examination of the unit cell and the discovery of additional symmetry elements. The structure was then refined according to C2/m, which gives improved refinement results.
- (12) Sheldrick, G. M. In *Crystallographic Computing 3*; Sheldrick, G. M., Krüger, C., Goddard, R., Eds.; Oxford University Press: London/New York, 1985; pp 175–189.

Table 2. Positional and Equivalent Displacement Parameters for Ba₂Cu(PO₄)₂

atom	<i>x</i>	<i>y</i>	<i>z</i>	<i>B</i> _{eq} ^a , Å ²
Ba	0.17377(3)	0	0.21462(6)	0.72(2)
Cu	0	1/2	1/2	0.69(4)
P	0.1334(1)	0	0.7019(3)	0.72(6)
O (1)	0.0467(4)	0	0.8235(7)	1.3(2)
O (2)	0.2548(4)	0	0.8419(7)	1.0(2)
O (3)	0.1219(3)	0.2442(6)	0.5630(5)	0.9(1)

^a Equivalent isotropic thermal parameters defined as *B*_{eq} = (8π²/3) trace *U*.

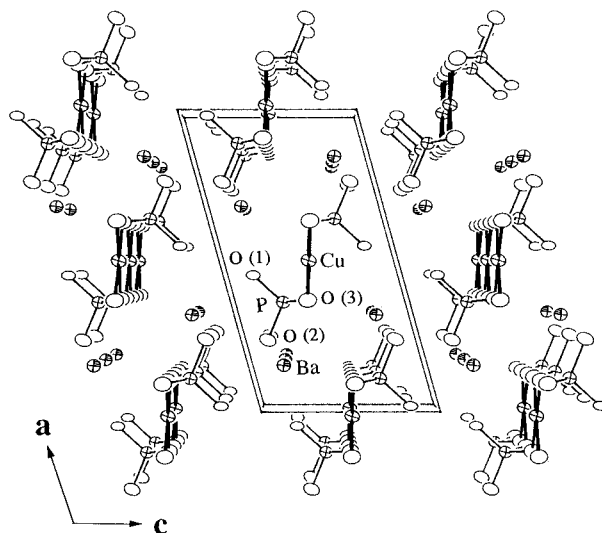


Figure 1. ORTEP perspective drawing of the Ba₂Cu(PO₄)₂ structure viewed along the *b* axis. The CuO₄ and PO₄ coordination geometries are outlined by thick and thin lines, respectively; the Ba–O bonds are omitted for clarity. The anisotropic thermal ellipsoids are drawn in 90% probability.

Infrared Spectroscopy. The infrared absorption spectra of the title compound was studied in the range of 1600–400 cm⁻¹ wavenumbers according to the procedures described in ref 3a. It showed a series of bands from 1110 to 950 cm⁻¹ and from 630 to 460 cm⁻¹ characteristic of *ν* (P–O) and *δ* (O–P–O) of PO₄, respectively.¹³

Magnetic Measurements. The magnetic susceptibility was measured using a Quantum Design SQUID MPMS-5S magnetometer. The measurements were carried out from 4.7 to 300 K in a field of 500 G. The powder sample (~26.5 mg) was contained in a gel capsule sample holder which was suspended in a straw from the sample translator drive. The temperature and field dependence of the susceptibility of the container were previously determined and their effect was negligible. The magnetic susceptibility was corrected for core diamagnetism with Pascal's constants, but not for temperature-independent paramagnetism.

Results and Discussion

Structure Description. The structure of the title compound is relatively simple compared to most copper(II) phosphate compounds and can be considered quasi-one-dimensional due to the [Cu(PO₄)₂]_∞ chain (see below). Figure 1 shows a perspective ORTEP¹⁴ drawing of the Ba₂Cu(PO₄)₂ structure viewed along the copper(II) phosphate chain. The barium cations (represented by ellipsoids with shaded octants) reside between the parallel chains and maintain the interchain connectivity through coordination to nine oxygen anions.

Figure 2a¹⁵ shows a partial structure of the copper phosphate chain, [Cu(PO₄)₂]_∞, which consists of an array of Cu²⁺ cations

(13) Nakamoto, K. *Infrared and Raman Spectra of Inorganic and Coordination Compounds*, 4th ed.; John Wiley and Sons, Inc.: New York, 1986.

(14) Johnson, C. K. ORTEP II. Report ORNL-5138; Oak Ridge National Laboratory: Oak Ridge, TN, 1976.

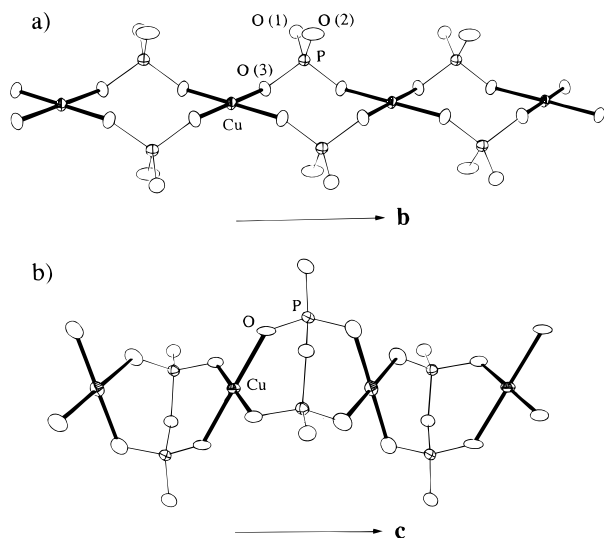


Figure 2. (a) Partial structure of the $[\text{Cu}(\text{PO}_4)_2]_\infty$ chain propagating along the b axis. Each PO_4 has two $\text{P}-\text{O}(3)$ bonds bridging a pair of Cu^{2+} cations and two other bonds, $\text{P}-\text{O}(1)$ and $\text{P}-\text{O}(2)$, exclusively bonded to Ba^{2+} (not shown). The anisotropic thermal ellipsoids are drawn in 90% probability. (b) For comparison, a single wave-like $[\text{CuP}_2\text{O}_7]_\infty$ chain in the $\text{Na}_2\text{CuP}_2\text{O}_7$ structure (see text).

Table 3. Important Bond Distances (Å) and Angles (deg) for $\text{Ba}_2\text{Cu}(\text{PO}_4)_2^a$

CuO ₄			
Cu—O(3) ^{a,b,c,d}	1.941(3) (4×)	O(3) ^{a,b} —Cu—O(3) ^{c/d}	85.2(2) (2×)
O(3) ^{a,b} —Cu—O(3) ^{c/d}	180.0 (2×)	O(3) ^{a/c} —Cu—O(3) ^{b/d}	94.8(2) (2×)
PO ₄			
P—O(1) ^a	1.511(6)	P—O(3) ^a	1.560(4)
P—O(2) ^a	1.533(5)	P—O(3) ^a	1.560(4)
O(1) ^a —P—O(2) ^a	110.4(3)	O(2) ^a —P—O(3) ^{a,c}	107.5(2) (2×)
O(3) ^a —P—O(3) ^a	106.9(3)	O(2) ^a —P—O(3) ^{a,c}	112.2(2) (2×)

^a Symmetry codes: (a) x, y, z ; (b) $-x, y, 1 - z$; (c) $-x, 1 + y, -z$; (d) $-x, 1 - y, 1 - z$; (e) $x, -y, z$

that are doubly bridged by PO_4 anions (Figure 2a). Both cations are four-coordinated with oxygen atoms in a square planar CuO_4 and tetrahedral PO_4 geometries. Each pair of bridging PO_4 tetrahedra are in a staggered configuration above and below the CuO_4 square plane. This arrangement results in the observed linear configuration with a long Cu—Cu separation distance 5.13 Å ($\equiv b$), which is far longer than the distance in elemental copper, 2.56 Å.¹⁶ The bond interactions in this chain are solely characterized by Cu—O—P—O—Cu linkages.

A close structural correlation can be drawn between $\text{Ba}_2\text{Cu}(\text{PO}_4)_2$ and $\text{Na}_2\text{CuP}_2\text{O}_7$ with respect to the copper phosphate chains. These two chemical formulae differ from each other by a single oxygen anion whose charge is balanced by the different electropositive cations, Ba^{2+} vs Na^+ . If one could imagine that the PO_4 pairs in Figure 2a are fused through a shared oxygen atom, the $[\text{Cu}(\text{PO}_4)_2]_\infty$ chain can be reformulated as $[\text{CuP}_2\text{O}_7]_\infty$, resulting the undulating chain structure observed in $\text{Na}_2\text{CuP}_2\text{O}_7$ (Figure 2b).

Table 3 lists selected bond distances for CuO_4 and PO_4 polyhedra. The Cu—O(3) bond distance is 1.94 Å, which is consistent with 1.93 Å, the sum of the Shannon crystal radii¹⁷

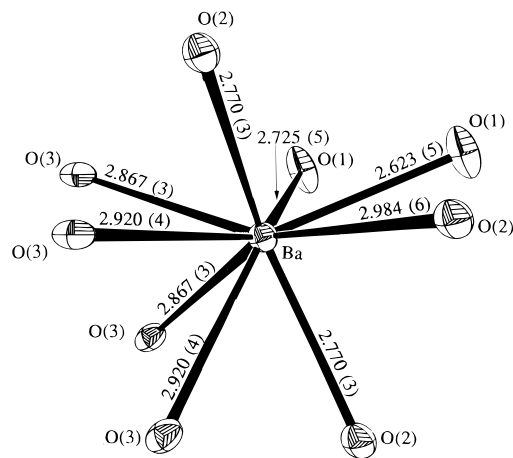


Figure 3. Drawing of a BaO_9 coordination geometry. The Ba—O bond distances are in angstroms and the anisotropic thermal ellipsoids are drawn in 90% probability.

for a four-coordinated Cu^{2+} and O^{2-} , and comparable with 1.91–1.96 Å of the $\text{Na}_2\text{CuP}_2\text{O}_7$ phase. The PO_4 bond distances are in the range of 1.51–1.56 Å, which is close to 1.55 Å, the sum of the Shannon crystal radii for a four-coordinate P^{5+} and O^{2-} . The bond valence sum (BVS) calculations¹⁸ based upon observed bond distances are consistent with the assigned formal oxidation states of the cations; the calculated valences for Cu^{2+} and P^{5+} cations are +1.92 and +4.87, respectively.

The barium cation resides in an irregular BaO_9 geometry, which can be seen in Figure 3. The Ba—O bond distances are quite diverse, ranging from 2.62–2.98 Å; this is due to the complex bond interaction occurring at each oxygen anion ($\text{O}(1)-2\text{Ba}/1\text{P}$; $\text{O}(2)-3\text{Ba}/1\text{P}$; $\text{O}(3)-2\text{Ba}/1\text{Cu}/1\text{P}$). The averaged Ba—O distance, 2.83 Å, however, matches closely with 2.85 Å, the sum of Shannon crystal radii for nine-coordinate Ba^{2+} (1.61 Å) and four-coordinate O^{2-} (1.24 Å). The BVS calculation for Ba^{2+} results in a value of +2.19.

It is interesting to realize that the title compound possesses the same bonding as $\text{Ba}_2\text{VO}(\text{PO}_4)_2 \cdot \text{H}_2\text{O}$ with respect to the linear chain. In the latter compound, the vanadium cation is octahedrally coordinated to oxygen. The four equatorial bonds are similar to the four Cu—O bonds found in the title compound; a short $\text{V}=\text{O}$ bond and a long $\text{V}-\text{O}$, which bond the vanadium atom to the water molecule, complete the octahedra. In other words, the copper cations in the $[\text{Cu}(\text{PO}_4)_2]_\infty$ chain of the title compound can be considered octahedrally coordinated with the apical positions vacant. Despite the difference in coordination of center cations, the corner-shared connectivity and relative orientation of the CuO_4/VO_6 to the PO_4 polyhedra are identical in the two chain structures. In light of the similarity in valence of the two cations, compounds based on $(\text{VO})^{2+}$ and Cu^{2+} may be an attractive pair for future correlation studies of their chemistry and structure. To our knowledge, this is the only pair of vanadyl and copper(II) phosphates where the extended structures adopt the same linear chains.

Magnetic Properties. Magnetic susceptibility data are plotted in Figure 4 as both molar susceptibility (χ) and χT vs temperature (T). The features of the χT vs T curve can be divided into three temperature regions. At the higher temperatures, ca. 190–300 K, a nearly perfect Curie–Weiss paramagnetic behavior is shown. The intermediate-temperature region, ca. 20–190 K, exhibits a gradual decrease in χT as the temperature is lowered, which indicates a weak antiferromagnetic coupling. Upon further cooling of the sample, the low-

(15) SHELXTL PC VERS. 4.1. Siemens Crystallographic Research Systems, Siemens Analytical X-Ray Instruments Inc., Madison, WI, 1990.

(16) Greenwood, N. N.; Earnshaw, A. *Chemistry of the Elements*; Pergamon Press: Oxford, England, 1984; pp 1366–1368.

(17) Shannon, R. D. *Acta Crystallogr.* **1976**, A32, 751.

(18) Brese, N.; O'Keefe, M. *Acta Crystallogr.* **1991**, B47, 192.

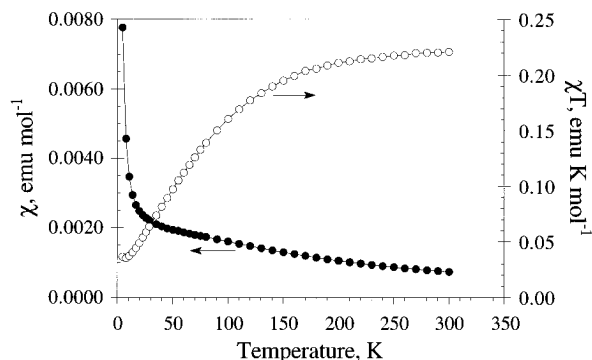


Figure 4. Susceptibility data for Ba₂Cu(PO₄)₂ plotted as χ and χT vs T .

temperature region, $T < 20$ K, is characterized by an increase in χT , suggesting a possible antiferro-to-ferromagnetic transition.

Further analysis shows that the paramagnetic region can be fitted with the Curie-Weiss equation, $\chi = C/(T - \Theta)$, giving rise to $C = 4.01 \times 10^{-1}$ (emu K)/mol, and $\Theta = -97.5$ K. The corresponding μ_{eff} is $1.79 \mu_{\text{B}}$, slightly higher than the ideal value for copper(II) of $1.73 \mu_{\text{B}}$. The negative Weiss constant suggests an antiferromagnetic-like ordering which is consistent with the downward progression of the χT vs T curve in the intermediate-temperature region. The ferromagnetic coupling with a transition observed at ca. 8 K was unexpected, as there are neither Cu–O–Cu nor short Cu–Cu bond interactions. This is, in fact, different than the antiferromagnetic behavior observed in the structurally related Ba₂(VO)(PO₄)₂·H₂O, where the magnetic ordering was rationalized as superexchange via V–O–P–O–V.⁷ A similar ferromagnetic behavior is evident, however, in the above mentioned 1D Na₂CuP₂O₇,¹⁹ where the Cu–Cu distance is 4.03 Å (shorter than 5.13 Å of the present structure) and the transition occurs at $T_c \sim 23$ K. A weak ferromagnetic coupling is also observed, at low temperatures, in BaCo₂Si₂O₇²⁰

and Cu₄(AsO₄)₂O²¹, where the structures contain 1-D Co–O chain and 2-D Cu–O sheet, respectively. It should be noted that this is the first example, thus far, where ferromagnetic coupling is observed in 1-D copper phosphate chains characterized by Cu–O–P–O–Cu linkages as stated above. This is unusual given the fact that the phosphate groups are intuitively considered closed-shell, nonmagnetic anions. It is tempting to suggest that the low-temperature ferromagnetic ordering is attributed to an interaction through space via copper pairs instead of the Cu–O–P–O–Cu linkages. But, it should be noted that, since a powder sample was used, the possibilities of incorporated ferromagnetic and/or paramagnetic impurities cannot be ruled out. Further studies into the nature of the magnetic coupling await large single crystals.

Summary

Eutectic halide fluxes provide a convenient media to allow novel low-dimensional phases to be isolated. Ba₂Cu(PO₄)₂ exhibits one-dimensional chain frameworks, which are rare in copper(II) phosphate compounds. The Cu²⁺ oxidation state is established by the study of BVS calculations and magnetic susceptibility. The structural correlation drawn with the vanadyl compound, Ba₂VO(PO₄)₂·H₂O, suggests that close attention should be paid in future studies of Cu²⁺- and (VO)²⁺-based phosphate chemistry. More novel structures and interesting magnetochemistry are forthcoming.

Acknowledgment. Support of this work from the National Science Foundation (Grant DMR-9208529) is gratefully acknowledged. Funds for the Rigaku AFC5S diffractometer and the SQUID magnetometer by the National Science Foundation are acknowledged. We thank Professor Jacobson for the useful discussion and the preprint of the article describing Ba₂VO(PO₄)₂·H₂O.

Supporting Information Available: Tables of detailed crystallographic data, anisotropic thermal parameters, and bond distances and angles (4 pages). Ordering information is given on any current masthead page.

IC9511783

(19) Etheredge, K. M. S.; Hwu, S.-J. Unpublished research, Rice University, 1995.

(20) Adams, R. D.; Layland, R.; Datta, T.; Rayen, C. *Polyhedron* **1993**, *12*, 2075.

(21) Adams, R. D.; Layland, R.; Rayen, C. *Inorg. Chem.* **1995**, *34*, 5397.